# Through-Bond Energy Transfer Cassettes for Multicolor Encoding

Xinfu Zhang, Yi Xiao,* Ling He, and Yuhui Zhang

State Key Laboratory of Fine Chemicals, Dalian University of Technology, Dalian 116024, China

S *Supporting Information*

ABSTRACT: Through-bond energy transfer (TBET) has been proposed as a versatile strategy to develop encoded microspheres. Together with the donor molecule, two TBET cassettes with high intramolecular TBET efficiencies (98% and 99%) and pseudo-Stokes shifts about 70 and 160 nm have been codoped into PS microspheres. Upon exclusive excitation at 480 nm, these microspheres emit simultaneously triple peaks at 512, 570, and 656 nm. Further confocal imaging and flow cytometric analysis demonstrates satisfactory performances of the new encoded microspheres.
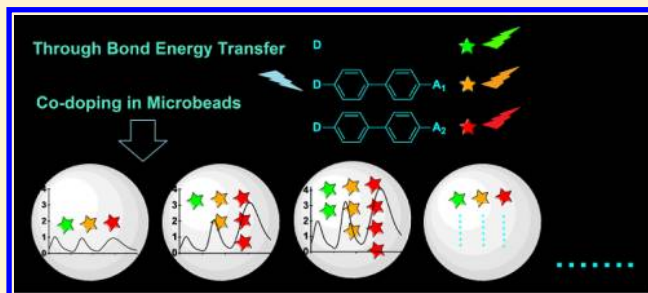
Flow fluorescence microspheres array is a high-throughput technique that can perform multiple discrete assays in a single tube. This detection combines the specificity of fluorescence-encoded microspheres and the high sensitivity of flow cytometry.[1] It is of great demand in both research and clinical applications, such as gene profiling, clinical diagnostics, and environmental analysis.[2,3] Although the concept of multicolor encoding has been proposed for nearly 20 years, the technical core of how to produce these uniform 5–10 μM microspheres is highly unpublicized, which is unfavorable for widespread applications.

It looks easy but is challenging to achieve single-excitation several-emissions, the essential requirement for multicolor encoding. Generally, two or more fluorophores with different and large Stokes shifts are the first choices.[4,5] Inorganic fluorophores, e.g., quantum dots (QDs), have been employed,[6] but limiting factors of QD, e.g., "blink" and their compatibility within biosystems, prevent them from widespread applications. A few large Stokes shift dyes with ICT (*intramolecular* charge transfer) nature had also been attempted, but they suffered from the broad emission and low excitation efficiency,[5] which decreases the sensitivity and accuracy. In contrast to QD and ICT dyes, most organic dyes with high fluorescence quantum yields have small Stokes shifts. Thus, for encoding microspheres excited at a single wavelength, it is almost impracticable for two fluorophores to emit in different spectral ranges independently. The practical way to mediate emission signatures should be fluorescence resonance energy transfer (FRET).

However, in practice, *intermolecular* FRET for fluorescence encoding is still imperfect. To obtain usable FRET efficiency, one of the preconditions is a considerable overlap of the emission band of donor and the absorption band of acceptor.[4,5] However, owing to the small Stokes shifts of most excellent fluorophores, the above-mentioned overlap is also accompanied by the hardly avoidable crosstalk of two emission bands. Another precondition for efficient FRET is the spatial distance between donor and acceptor should be as short as possible (less

than 10 nm).[7,8] However, within the microspheres, there is no guarantee of the sufficiently short distances. In addition, because of the randomness in dyes' distributions, the *intermolecular* FRET efficiencies are not stable in different batches of microspheres and so the fluorescence coding is not repeatable.

To overcome the problems of *intermolecular* FRET encoding mode, we propose a platform approach to three-color fluorescence encoded microspheres by codoping two *intramolecular* through-bond energy transfer (TBET) cassettes and the donor. In a so-called TBET cassette, the donor dye and the acceptor are connected by a rigid, short, and conjugated linker, which makes the excitation energy-transfer processes "through bond".[9–11] First, TBET is not subjected to the constraint of spectral overlap between the donor emission and the acceptor absorption, which means TBET cassettes may have very large pseudo-Stokes shifts.[11,12] Second, TBET occurs extremely fast (in picosecond or even femtosecond range) and highly efficiently (approaching 100%), which is not as severely affected by surrounding medium molecules as FRET is. Burgess et al.[9,10,12] and Akkaya et al.[13,14] did the pioneering work on construction of TBET cassettes, and Ziessel et al.,[15,16] Lin,[11] our group,[17,18] and others[19,20] adopted this concept to design ratiometric probes and solar energy harvesters. Very recently, we and co-workers[21,22] had extended this concept to develop multiply pumped laser dyes with unprecedented laser performance. Inspired by these previous works, especially by Akkaya et al., who proposed the strategy for higher TBET effciency,[13] we clearly know TBET cassettes' photophysical features, such as its large pseudo-Stokes shift and stable and high energy transfer efficiency,[23] are exactly what we desire for fluorescence coding microspheres.

Herein, two TBET cassettes, **BDP-A1** and **BDP-A2**, were prepared efficiently (Figure 1a). Three BODIPY derivatives
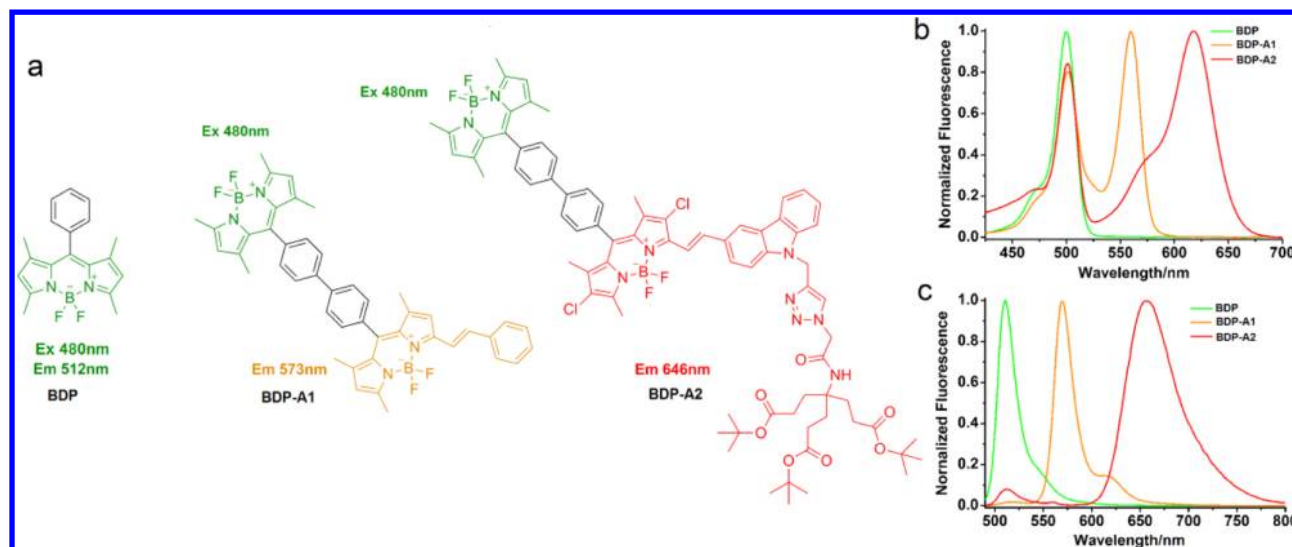
Figure 1. (a) Structures of three fluorophores **BDP**, **BDP-A1**, and **BDP-A2**. Normalized (b) absorption and (c) fluorescence spectra of three fluorophores in THF.

Table 1. Photophysical Properties of BDP, BDP-A1, and BDP-A2 in THF

solvent	λ_{abs} (nm)	λ_{em} (nm)	ε (M^{-1} cm^{-1})	$\Phi_f{}^a$	Φ_d	ETE^e (%)	$R_0{}^f$ (Å)	R^g (Å)	ETE^h (%)
BDP	502	512	69200	0.77	0.77				
BDP-A1	502, 561	512, 570	71300, 87600	0.83^b, 0.78^c	0.015	98.1	83.52	10.35	99.9
BDP-A2	502, 618	512, 656	73200, 92400	0.35^b, 0.29^d	0.007	99.1	70.76	10.35	99.9

^{a}Rhodamine B is used as standard (Φ_f 0.69, in methanol). ^{b}Exciting wavelength, λ_{ex} = 480 nm. $^c\lambda_{ex}$ = 540 nm. $^d\lambda_{ex}$ = 580 nm. ^{e}Energy transfer efficiency, ETE =1-Φ_d/Φ_{d0}, Φ_d is the quantum yield of donor part in **BDP-A1** or **BDP-A2**, F_{d0} is the quantum yield of **BDP**. ^{f}Förster radius, calculated according to the equation, $R_0 = 0.211[k^2 n^{-4}\Phi_D \int_0^\infty I_D(\lambda)\varepsilon_A(\lambda)\lambda^4 d\lambda]^{1/6}$ k^2 = 2/3, n (THF) = 1.4050. ^{g}Radius, distance between the D and A groups (estimated using standard bond lengths). ^{h}Calculated according to the equation ETE = $R_0{}^6/[R_0{}^6 + R^6]$.
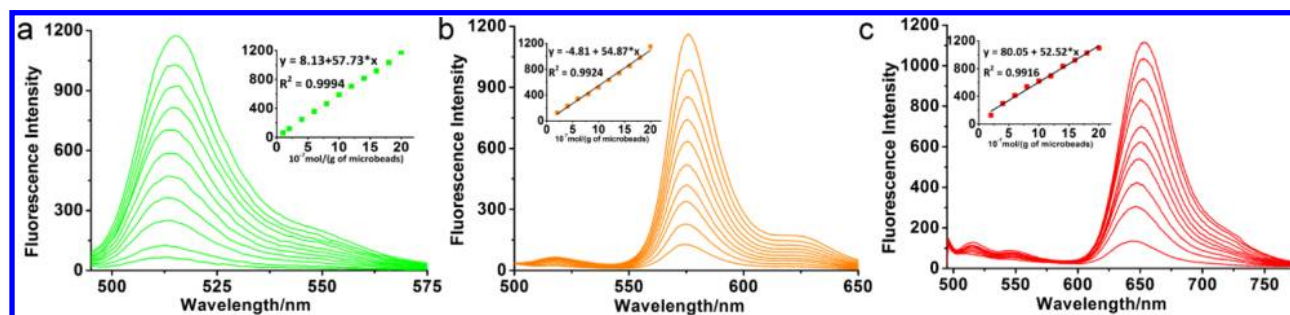

Figure 2. Fluorescence spectra changes (λ_{ex} = 480 nm) of singly labeled microspheres (in water) against doping amount. Inset: intensity of emission maxima vs doping amount, unit 10^{-7} mol/(g of microspheres). (a) For **BDP**, slit 1 nm, 2.5 nm; (b) for **BDP-A1**, slit 2.5 nm, 2.5 nm; (c) for **BDP-A2**, slit 5 nm, 2.5 nm.

with well-separated emission bands are chosen to construct the cassettes. A biphenyl group is adopted as a linker for consistent and highly efficient TBET according to our previous results.[22] In the case of poor solubility for **BDP-A2** due to its relatively large conjugation structure, a Newkome dendrimer is introduced. Figure 1b shows the absorbance spectra of the cassettes are essentially equal to the sum of donor and acceptor parts. They both maintain high molar extinction coefficients for the donor part ($\sim$73200 M^{-1} cm^{-1}). Upon excitation of three fluorophores at 480 nm, sharp fluorescence with different colors (512 nm, 570 and 656 nm) is observed (Figure 1c and Table 1). These emission spectra show very small overlap with each other. For **BDP-A1** and **BDP-A2**, they emit predominantly from their acceptor fragments. The emission peaks are very weak from donor at 512 nm. The quantum yields of **BDP-A1** are measured to be 0.83 and 0.78 for two different excitation

wavelengths (480 and 540 nm). **BDP-A2** shows a similar result with two quantum yields as 0.35 and 0.29 excited at 480 and 580 nm, respectively. That is to say, the fluorescence quantum yields do not vary significantly with excitation wavelength, which suggests almost complete energy transfer from donor to acceptor. Calculated values of energy-transfer efficiency (ETE) by two methods are listed in Table 1. Both methods provide high ETE values over 98% for **BDP-A1** and 99% for **BDP-A2**. In addition, these fluorophores show good solubility in a broad variety of organic solvents and they are proven as environmental factor-independent fluorophores.

Microspheres labeled by **BDP**, **BDP-A1**n or **BDP-A2** singly show linearly increases in emission intensity against the doping amount: (2−20) × 10^{-7} mol/(g of microspheres) as recorded in Figure 2. Good linear correlation is observed in each case. Importantly, upon excitation of microspheres singly labeled by

two cassettes at 480 nm (absorption of donor) the emission of donor at 512 nm is ignorable, compared with the intensive emissions from the acceptors. Thus, the TBET efficiencies in microspheres are still very high. Further studies on excitation spectra give a consistent result (Figure S1, Supporting Information) that TBET cassettes can be efficiently excited at the absorption of donor. Thus, properties of singly labeled microspheres indicate that **BDP-A1** and **BDP-A2** are ideal modules for fluorescence encoding microspheres.

Triply doped microspheres exhibit controllable emission signatures along with the changes in doping amounts of **BDP**, **BDP-A1**, and **BDP-A2**. Three fluorophores are successfully codoped into microspheres under a same doping procedure (for dye loading amounts, see Table S1, Supporting Information). Non-normalized fluorescent spectra of fluorescence coding microspheres dispersed in water are shown in Figure 3. The spectra show three clearly separated emission
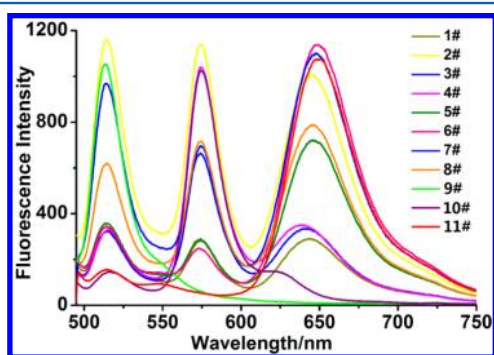

Figure 3. Fluorescence spectra of triple labeled microspheres in water (λ_{ex} = 480 nm, λ_{em} = 490−750 nm, slit 5 nm, 5 nm).

peaks, which is a result that previous methods cannot achieve. The doping amount of each fluorophore is adjusted at three levels (just for illustration; no problem for more levels), and thus, there are three levels of intensity changes for each emission maximum. Moreover, under a same labeling operation, intensity of each emission maximum shows a relative stable value against doping amount. That is to say, we can adjust the intensity of each emission maximum simply by increasing or decreasing the amount of corresponding fluorophore without affecting the others' emissions. Thus, fluorescence coding microspheres based on TBET cassette exhibit tailored emission fingerprints other than a "this is it" result.

For better demonstrating the advantage of TBET cassette over conventional *intermolecular* FRET dye pair, we also labeled microspheres by the detached donor and acceptor. Here, we choose the second acceptor **A2** promising a larger pseudo-Stokes shift. No surprise, the result shows quite low FRET efficiency. In the experiment of codoping a fixed amount of **A2** [20×10^{-7} mol/(g of microspheres)] and a varied amount of donor **BDP** [$0-20 \times 10^{-7}$ mol/(g of microspheres)] in microspheres, emission spectra show only a very slight increase of **A2**'s emission intensity despite the remarkable and linear increase of the emission of donor (Figure 4). The inset clearly shows the different increasing trends of the two emission maxima. Furthermore, in another experiment of codoping a fixed amount of donor **BDP** and a varied amount of **A2**, spectra show moderate energy transfer from **BDP** to **A2** when the amounts of acceptor become large. However, to obtain equal emission intensity between **BDP** and **A2**, a large amount of **A2** up to 64×10^{-7} mol/(g of microspheres) is used. That is quite a high doping concentration and brings about a clear red shift of emission and a trend of fluorescence self-quenching. Hence, the low *intermolecular* FRET efficiency results in unsatisfactory tunability of donor−acceptor emission ratio, which is unfavorable for fluorescence encoding.

Confocal microscope images intuitively illustrate the encoding results. We set three channels to collect three emissions from **BDP**, **BDP-A1**, and **BDP-A2**, respectively. In Figure 5, there are six different microspheres that show different emission intensities in three channels (dye loading amounts, see Table S2, Supporting Information). For example, microspheres 1 and 5 are marked with their emissions (for others, see Figure S4, Supporting Information). Microspheres 1 are singly labeled with **BDP**, which shows bright fluorescence in green channel but no fluorescence in the other two channels. It demonstrates nearly no crosstalk between channels. Microspheres 5 codoped with three fluorophores exhibit fluorescence signals in all the three channels. Not only can the beads be easily distinguished by the color difference, but in addition, their encoding information can be readily demonstrated by emission fingerprints extracted from the microscopic images. As discussed previously, this type of simultaneous excitation with well-separated emissions is hardly possible for microspheres loaded with conventional organic dyes.

Flow cytometric analysis also confirms that these fluorescence encoded microspheres are suitable for high throughput assays. In two-color flow cytometric analysis, the fluorescence intensity ratio from different channel is the basis for the recognition of different fluorescent microspheres. Thus,
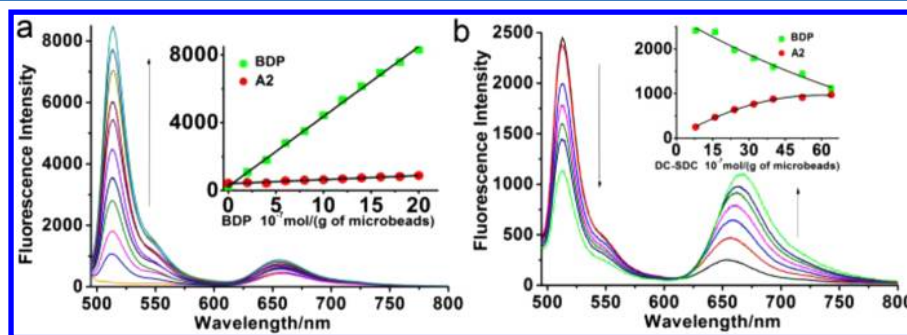

Figure 4. Fluorescence spectra changes of microspheres (in water, λ_{ex} = 480 nm) labeled by **BDP** (λ_{em} = 512 nm) and **A2** (λ_{em} = 656 nm). (a) Fluorescence spectra change vs doping amount of **BDP**, inset: intensity of emission maxima vs amount of **BDP**. (b) Fluorescence spectra change vs doping amount of **A2**. Inset: intensity of emission maxima vs amount of **A2**; unit 10^{-7} mol/(g of microspheres).
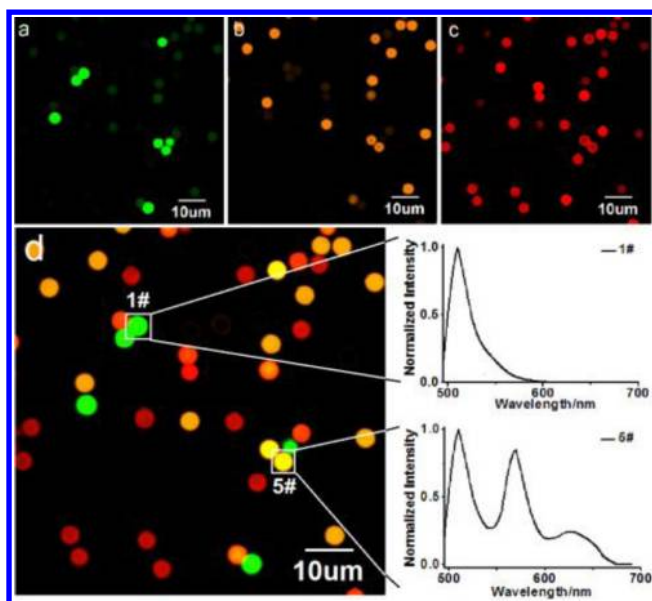
Figure 5. Confocal microscope images of triply doped fluorescence microspheres (λ_{ex} = 488 nm): (a) green channel (λ_{em} = 495−555 nm); (b) orange channel (λ_{em} = 560−620 nm); red channel (λ_{em} = 655−755 nm); (d) overlap of a, b, and c.

different emissions with small spectral crosstalk makes quantification of intensity from different channels easy, which means a precise ratio, namely, a precise decoding. Five randomly chosen microspheres with different I_{512}/I_{570} ratios (0.05, 2, 2.5, 7.5, and 10) adjusted by codoping different amounts of **BDP** and **BDP-A1** (Figures S5 and S6, dye loading amounts, Table S3, Supporting Information) are studied as representatives. The data dots for each group of microspheres are mostly distributed in linear banding regions that show similar slopes close to 1, which indicates that in each group all microspheres present an equable I_{512}/I_{570}, namely, that they are evenly labeled by the identical ratio of **BDP** to **BDP-A1** (Figure S6, Supporting Information). Interestingly, as shown in Figure 6a, the mixture of the above microspheres exhibits five clearly separated banding regions parallel to each other without overlapping, which indicates that differently encoded beads can be readily discriminated by a flow cytometer. The same experiment is also conducted by using microspheres with different codoping amounts of **BDP-A1** and **BDP-A2**. Micro-
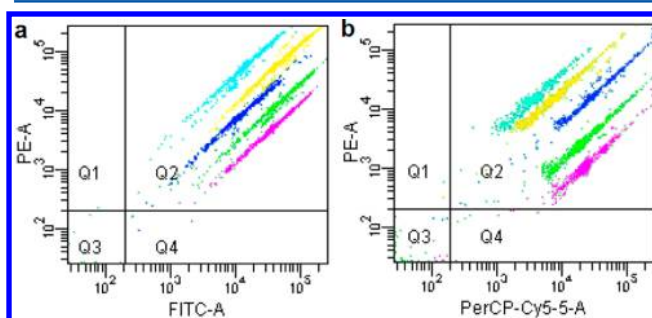

Figure 6. Flow cytometric analysis of a mixture sample of five microspheres: (a) co-doping by **BDP** and **BDP-A1**, FITC-A is the name for green channel: 530 ± 30 nm; PE-A is the name for red channel: 585 ± 42 nm; (b) co-doping by **BDP-A1** and **BDP-A2**, PE-A is the name for red channel: 585 ± 42 nm; PerCP-Cy5.5-A is the name for NIR channel: 670LP.

spheres with different I_{656}/I_{570} ratios can also be discriminated by a flow cytometer (Figure 6b). Flow cytometric analysis of five microspheres labeled by different amounts of **BDP-A1** and **BDP-A2** is given in the Supporting Information (Figures S7 and S8, dye loading amounts, Table S4).

In conclusion, the TBET cassette strategy has been proposed for rational development of encoded microspheres for the first time. By the connections of two different long wavelength BODIPY dyes to a short wavelength BODIPY dye via a biphenyl linker, two TBET cassettes have been constructed. Together with the donor they are loaded into self-produced polystyrene microspheres which demonstrate tailored emission fingerprints upon single excitation of the donor. The good fluorescence encoding performance should be ascribed to the high efficiency of TBET. In contrast, within those microspheres loaded with unbound donor and acceptor, the encoding performance is unsatisfactory, resulted from the poor efficiency of *intermolecular* FRET. Confocal imaging and flow cytometric analysis demonstrates that the TBET-based encoded microspheres are of practical applicability in multiplex and high throughput assays. Since there are a variety of excellent dyes as candidates for donors and acceptors, above TBET strategy is a versatile approach for DIY production of fluorescence encoded microspheres by researchers.

■ EXPERIMENTAL SECTION

Microsphere Synthesis and Fluorophore Doping. Monodisperse polystyrene microspheres, with carboxy group outside, are prepared by two-stage dispersion polymerization. These microspheres are monodisperse and uniform in size (∼5.5 μm) (Figure S2, Supporting Information), which is usually required for a flow cytometric measurement.[24,25] Scanning electron microscope revealed that the beads had a 5.5 μm diameter in size (diameter). Incorporation of three fluorophores is achieved by swelling the beads in a solvent mixture containing 22% (v/v) THF and 78% (v/v) H_2O and by adding a controlled amount of fluorophores to the mixture (FigureS3, Supporting Information). Fluorophores were prepared as a 1 mM solution in THF. After 4 min, the embedding process was completed by adding a large amount of water followed by centrifugation to obtain the fluorescence microspheres. The beads were washed with ethanol twice in case unlabeled dyes were present.

Synthesis of Compounds. The BDP,[26] DC-SPC,[26] 4′-B-BODIPY,[27] and Newkome dendrimer[28] were prepared following the reported methods. For others, see below:
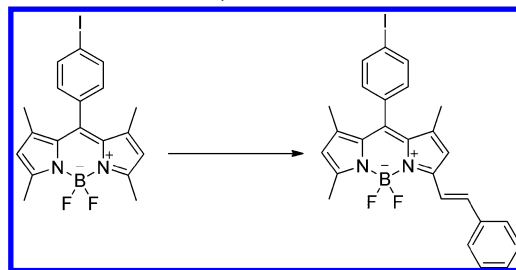

A1. BDP (1.11 mmol, 500 mg) and benzaldehyde (1.11 mmol, 118 mg) were added to a 100 mL round bottomed flask containing 50 mL of toluene, and to this solution were added piperidine (1 mL) and acetic acid (1 mL). The mixture was heated under reflux by using a Dean−Stark trap, and reaction was monitored by TLC 1:5 CH_2Cl_2/hexanes (R_f 0.3). When all the starting material had been consumed, the mixture was cooled to room temperature and solvent was evaporated. Water (300 mL) was added to the residue, and the product was extracted into the CH_2Cl_2 (3 × 200 mL). The organic phase was dried over Mg_2SO_4 and evaporated, and the residue was purified by silica gel column chromatography using 1:5 CH_2Cl_2/hexanes as the eluent to yield the desired product **A1** as a purple

powder (179 mg, 30%): mp 261−263 °C; ^{1}H NMR (400 MHz, CDCl$_3$) δ 7.86 (d, 2H), 7.67 (d, 1H), 7.59 (d, 2H), 7.37 (t, 2H), 7.30 (t, 1H), 7.25 (d, 1H), 7.08 (d, 1H), 6.62 (s, 1H), 6.02 (s, 1H), 2.59 (s, 3H), 1.47 (s, 3H), 1.44 (s, 3H); ^{13}C NMR (100 MHz, CDCl$_3$) δ 156.0, 152.9, 142.7, 138.9, 138.3, 136.5, 136.3, 134.6, 130.2, 128.9, 128.7, 127.5, 121.6, 119.1, 117.7, 94.7, 14.9, 14.7, 14.7; MS m/z (TOF MS ES) calcd M$^+$ for C$_{26}$H$_{22}$BN$_2$F$_2$I 538.0889, found 538.0851.
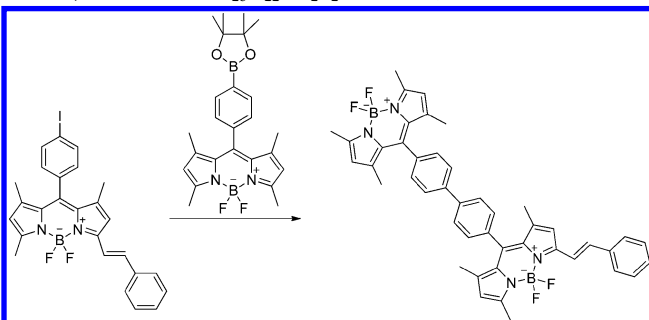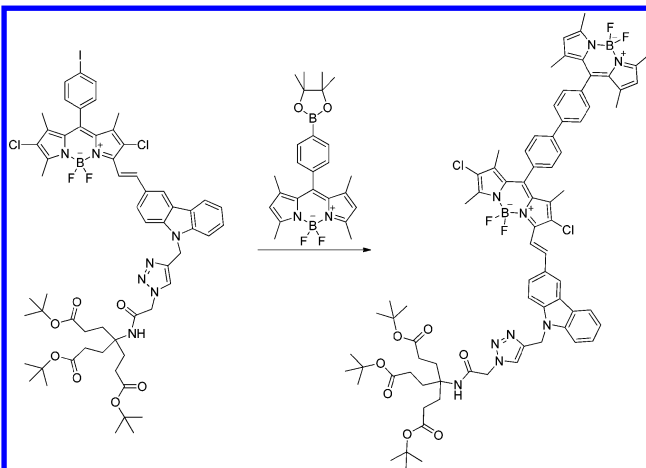

BDP-A1. A1 (0.19 mmol, 100 mg), **4′-B-BODIPY** (0.19 mmol, 86 mg), PPh$_3$ (4.9 mg, 0.019 mmol), Pd(OAC)$_2$ (6.6 mg, 0.03 mmol), Na$_2$CO$_3$ (42 mg, 0.4 mmol), n-propanol/THF/water (3 mL/6 mL/0.3 mL), and a magnetic stir bar were placed in a 25 mL round-bottom flask under a nitrogen atmosphere. The mixture was heated at 75 °C for 3 h. Then the crude product was purified through silica gel column chromatography with a mixture of 1:4 CH$_2$Cl$_2$/hexanes as eluent. A brown solid was obtained (128 mg, 92%): mp >300 °C; ^{1}H NMR (400 MHz, CDCl$_3$) δ 7.83 (d, 4H), 7.61 (d, 1H), 7.59 (d, 2H), 7.44−7.37 (m, 6H), 7.30 (t, 1H), 7.26 (d, 1H), 6.64 (s, 1H), 6.04 (s, 1H), 6.01 (s, 2H), 2.62 (s, 3H), 2.58 (s, 6H), 1.54 (s, 3H), 1.50 (s, 3H),1.48 (s, 6H); ^{13}C NMR (100 MHz, CDCl$_3$) δ 155.9, 155.7, 152.7, 151.0, 143.0, 142.9, 142.2, 141.2, 140.7, 140.0, 136.5, 136.1, 134.7, 132.8, 131.9, 131.4, 129.0, 128.8, 128.7, 127.6, 127.5, 14.9, 14.7, 14.7, 14.6; MS m/z (TOF MS ES) calcd M$^+$ for C$_{45}$H$_{40}$B$_2$N$_4$F$_4$ 734.3375, found 734.3348.
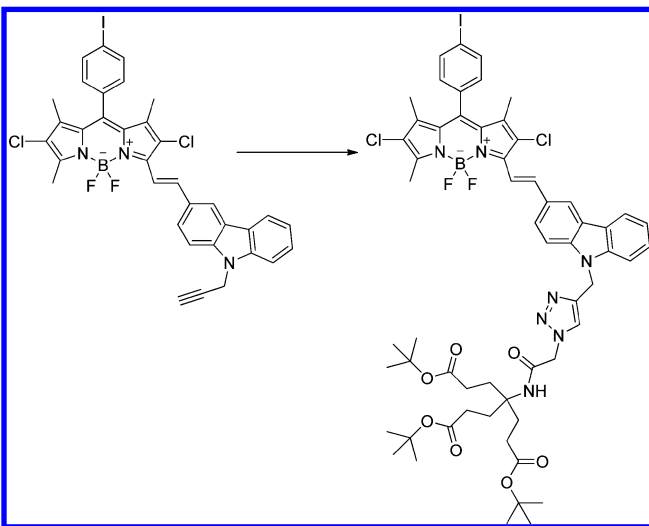
A2. Under a nitrogen atmosphere, CuSO$_4$·5H$_2$O (2.8 mg, 0.012 mmol) in H$_2$O (1 mL) and Na−ascorbate (4.2 mg, 0.022 mmol) in H$_2$O (1 mL) followed by DIPEA (30 mL, 0.174 mmol) were added to a solution of Newkome dendrimer (52 mg, 0.106 mmol) in EtOH (8 mL). Then a solution of **DC-SPC** (63 mg, 0.086 mmol) in toluene (20 mL) was slowly added dropwise to the mixture in the absence of light. The reaction mixture was stirred in the dark for 12 h at rt. Still in the absence of light, the solvent was evaporated off under vacuum, and the product was purified by silica gel column chromatography using 2:1 hexanes/ethyl acetate as the eluent yielded the desired product **A2** as dark blue solid (100 mg, 95%): mp 167−169 °C; ^{1}H NMR (400 MHz, CDCl$_3$) δ 8.30 (d, 1H), 8.25 (s, 1H), 8.15 (d, 1H), 7.99 (d, 2H), 7.80−7.70 (m, 2H), 7.53 (d, 2H), 7.48 (t, 3H), 7.37 (s, 1H), 7.29 (d, 1H), 7.05 (d, 2H), 6.74 (s, 1H), 5.66 (s, 2H), 4.80 (s, 2H), 2.65 (s,

3H), 2.14 (t, 6H), 1.91 (t, 6H), 1.65 (s, 3H), 1.45 (s, 3H), 1.41 (s, 27H); ^{13}C NMR (100 MHz, CDCl$_3$) δ 172.9, 163.9, 141.0, 140.6, 138.6, 134.1, 130.1, 128.7, 126.5, 126.0, 123.8, 123.2, 120.8, 120.7, 120.2, 109.3, 109.2, 95.4, 81.0, 58.2, 53.2, 39.0, 30.0, 29.6, 28.1, 12.6, 12.2; MS m/z (TOF MS ES) calcd M$^+$ for C$_{59}$H$_{67}$BN$_7$O$_7$F$_2$NaCl$_2$I 1254.3483, found 1254.3463.

BDP-A2. A2 (0.08 mmol, 100 mg), **4′-B-BODIPY** (0.08 mmol, 36 mg), PPh$_3$ (4.9 mg, 0.019 mmol), Pd(OAC)$_2$ (6.6 mg, 0.03 mmol), Na$_2$CO$_3$ (21 mg, 0.2 mmol), n-propanol/THF/water (3 mL/6 mL/0.2 mL), and a magnetic stir bar were placed in a 25 mL round-bottom flask under a nitrogen atmosphere. The mixture was heated at 75 °C for 3 h. Then the crude product was purified through silica gel column chromatography with a mixture of 1:2 hexanes/ethyl acetate as eluent. A dark blue solid was obtained (99 mg, 85%): mp 215−216 °C; ^{1}H NMR (400 MHz, CDCl$_3$) δ 8.37 (d, 1H), 8.26 (s, 1H), 8.16 (d, 1H), 7.84 (s, 4H), 7.79 (d, 1H), 7.74 (s, 1H), 7.53 (d, 2H), 7.48 (t, 1H), 7.43−7.38 (m, 5H), 7.28 (d, 1H), 6.74 (s, 1H), 6.01 (s, 2H), 5.66 (s, 2H), 4.80 (s, 2H), 2.67 (s, 3H), 2.58 (s, 6H), 2.15 (t, 6H), 1.92 (t, 6H), 1.66 (s, 3H), 1.52 (s, 3H), 1.49 (s, 6H), 1.48 (s, 3H), 1.42 (s, 27H); ^{13}C NMR (100 MHz, CDCl$_3$) δ 172.8, 163.8, 155.7, 151.8, 148.3, 144.3, 143.0, 141.1, 141.0, 140.6, 138.4, 139.8, 139.0, 136.8, 134.7, 134.1, 131.4, 130.7, 128.9, 128.8, 128.7, 127.8, 127.6, 126.5, 125.9, 123.7, 123.1, 121.3, 120.8, 120.6, 120.1, 109.3, 109.2, 80.9, 58.2, 53.1, 38.9, 29.9, 29.7, 14.7, 12.6, 12.2; MS m/z (TOF MS ES) calcd M$^+$ for C$_{78}$H$_{85}$B2N$_9$O$_7$F$_4$NaCl$_2$ 1450.5969, found 1450.5920.

■ ASSOCIATED CONTENT

ⓢ Supporting Information

Experimental procedures, characterization and additional spectra. This material is available free of charge via the Internet at http://pubs.acs.org.

■ AUTHOR INFORMATION

Corresponding Author

*E-mail: xiaoyi@dlut.edu.cn.

Notes

The authors declare no competing financial interest.

■ ACKNOWLEDGMENTS

■ REFERENCES

(1) Fulton, R. J.; McDade, R. L.; Smith, P. L.; Kienker, L. J.; Kettman, J. R. Clin. Chem. **1997**, 43, 1749−1756.

(2) Yuan, P. F.; Ma, Q.; Meng, R. Z.; Wang, C.; Dou, W. C.; Wang, G. N.; Su, X. G. *J. Nanosci. Nanotechnol.* **2009**, *9*, 3092−3098.

(3) Wang, H. Q.; Wang, J. H.; Li, Y. Q.; Li, X. Q.; Liu, T. C.; Huang, Z. L.; Zhao, Y. D. *J. Colloid Interface Sci.* **2007**, *316*, 622−627.

(4) Wang, L.; Tan, W. H. *Nano Lett.* **2006**, *6*, 84−88.

(5) Wu, W.-B.; Wang, M.-L.; Sun, Y.-M.; Huang, W.; Cui, Y.-P.; Xu, C.-X. *Opt. Mater.* **2008**, *30*, 1803−1809.

(6) Han, M.; Gao, X.; Su, J. Z.; Nie, S. *Nat. Biotechnol.* **2001**, *19*, 631−635.

(7) Zhang, X. l.; Xiao, Y.; Qian, X. H. *Org. Lett.* **2008**, *10*, 29−32.

(8) Yilmaz, M. D.; Bozdemir, A.; Akkaya, E. U. *Org. Lett.* **2006**, *8*, 2871−2873.

(9) Burghart, A.; Thoresen, L. H.; Chen, J.; Burgess, K.; Bergström, F.; Johansson, L. B.-A. *Chem. Commun.* **2000**, 2203−2204.

(10) Jiao, G.-S.; Thoresen, L. H.; Burgess, K. *J. Am. Chem. Soc.* **2003**, *125*, 14668−14669.

(11) Lin, W. Y.; Yuan, L.; Cao, Z. M.; Feng, Y. M.; Song, J. Z. *Angew. Chem., Int. Ed.* **2010**, *49*, 375−379.

(12) Ueno, Y.; Jose, J.; Loudet, A.; Pérez-Bolvar, C.; Anzenbacher, P.; Burgess, K. *J. Am. Chem. Soc.* **2011**, *133*, 51−55.

(13) Coskun, A.; Akkaya, E. U. *J. Am. Chem. Soc.* **2006**, *128*, 14474−14475.

(14) Guliyev, R.; Coskun, A.; Akkaya, E. U. *J. Am. Chem. Soc.* **2009**, *131*, 9007−9013.

(15) Ziessel, R.; Harriman, A. *Chem. Commun.* **2011**, *47*, 611−631.

(16) Ziessel, R.; Ulrich, G.; Haefele, A.; Harriman, A. *J. Am. Chem. Soc.* **2013**, *135*, 11330−11344.

(17) Yu, H. B.; Xiao, Y.; Guo, H. Y.; Qian, X. H. *Chem.—Eur. J.* **2011**, *17*, 3179−3191.

(18) Yu, H. B.; Jin, L. J.; Dai, Y.; Li, H. Q.; Xiao, Y. *New J. Chem.* **2013**, *37*, 1688−1691.

(19) Qu, X. Y.; Liu, Q.; Ji, X. N.; Chen, H. C.; Zhou, Z. K.; Shen, Z. *Chem. Commun.* **2012**, *48*, 4600−4602.

(20) Gong, Y. J.; Zhang, X. B.; Zhang, C. C.; Luo, A. L.; Fu, T.; Tan, W. H.; Shen, G. L.; Yu, R. Q. *Anal. Chem.* **2012**, *84*, 10777−10784.

(21) Xiao, Y.; Zhang, D. K.; Qian, X. H.; Costela, A.; García-Moreno, I.; Martín, V.; Pérez-Ojeda, M. E.; Bañuelos, J.; Gartzia, L.; López Arbeloa, I. *Chem. Commun.* **2011**, *47*, 11513−11515.

(22) Gartzia-Rivero, L.; Yu, H. B.; Bañuelos, J.; López-Arbeloa, I.; Costela, A.; Garcia-Moreno, I.; Xiao, Y. *Chem.—Asian J.* **2013**, *8*, 3133−3141.

(23) Fan, J. L.; Hu, M. M.; Zhan, P.; Peng, X. J. *Chem. Soc. Rev.* **2013**, *42*, 29−43.

(24) Ugelstad, J.; Kaggerud, K. H.; Hansen, F. K.; Berge, A. *Mukromol. Chem.* **1979**, *180*, 737−744.

(25) Ugelstad, J.; Mork, P. C.; Kaggerud, K. H.; Ellingsen, T.; Berge, A. *Adv. Colloid Interface Sci.* **1980**, *13*, 101−140.

(26) Zhang, X. F.; Xiao, Y.; Qi, J.; Qu, J. L.; Kim, B.; Yue, X. L.; Belfield, K. D. *J. Org. Chem.* **2013**, *78*, 9153−9160.

(27) Sekiya, M.; Umezawa, K.; Sato, A.; Citterio, D.; Suzuki, K. *Chem. Commun.* **2009**, 3047−3049.

(28) Newkome, G. R.; Kim, H. J.; Moorefield, C. N.; Maddi, H.; Yoo, K. *Macromolecules* **2003**, *36*, 4345−4354.